

# UC Riverside

## UC Riverside Previously Published Works

### Title

Random design of microfluidics.

### Permalink

<https://escholarship.org/uc/item/6f95v6rz>

### Journal

Lab on a chip, 16(21)

### ISSN

1473-0197

### Authors

Wang, Junchao

Brisk, Philip

Grover, William H

### Publication Date

2016-10-01

### DOI

10.1039/c6lc00758a

Peer reviewed



## Random design of microfluidics†

Cite this: DOI: 10.1039/c6lc00758a

 Junchao Wang,<sup>a</sup> Philip Brisk<sup>b</sup> and William H. Grover<sup>\*a</sup>

 Received 14th June 2016,  
Accepted 28th September 2016

DOI: 10.1039/c6lc00758a

[www.rsc.org/loc](http://www.rsc.org/loc)

In this work we created functional microfluidic chips without actually designing them. We accomplished this by first generating a library of thousands of different random microfluidic chip designs, then simulating the behavior of each design on a computer using automated finite element analysis. The simulation results were then saved to a database which a user can query via <http://random.groverlab.org> to find chip designs suitable for a specific task. To demonstrate this functionality, we used our library to select chip designs that generate any three desired concentrations of a solute. We also fabricated and tested 16 chips from the library, confirmed that they function as predicted, and used these chips to perform a cell growth rate assay. This is one of many different applications for randomly-designed microfluidics; in principle, any microfluidic chip that can be simulated could be designed automatically using our method. Using this approach, individuals with no training in microfluidics can obtain custom chip designs for their own unique needs in just a few seconds.

## 1 Introduction

Since the emergence of the first lab-on-a-chip devices in the late 1970s,<sup>1</sup> microfluidic chips have found applications in a variety of fields. But while the range of possible applications for microfluidics has blossomed, the process of designing microfluidic chips has remained relatively unchanged since the 1970s. Researchers still design new microfluidic chips by hand, drawing on a computer a design that represents a “best guess” of the desired functionality, then fabricating and testing the chip. If the chip does not perform as intended, the researcher alters the chip design and fabricates and tests the new chip. This iterative design process can take months or even years to yield a functional microfluidic chip. The inefficiency of this process slows the development of new microfluidic chips for important applications in research and healthcare. It also creates a significant barrier to entry for researchers who may wish to create custom microfluidic chips but are not microfluidics experts. Finally, the current design process only explores a tiny fraction of the many possible designs for microfluidic chips. It is reasonable to assume that there are many microfluidic chip designs that are better than our current designs, but these better designs will never be dis-

covered simply because our design process is too slow and inefficient.

Computers can help with the process of microfluidic chip design, but they have not yet completely automated the design process. For example, finite element analysis (FEA) software is sometimes used to simulate the behavior of a microfluidic chip before fabricating it. However, to use FEA software, a researcher still needs to create a chip design first; the software does not design the chip for them. Additionally, the cost of FEA software (\$7995 for a single-user license to the popular simulation tool COMSOL Multiphysics) is a practical barrier to widespread use of this software in microfluidics. Recently, software and algorithms from computer science and electrical engineering have been applied to microfluidic chip design with encouraging results. For example, the principles of semiconductor electronic design automation (EDA) can be leveraged to automatically design microfluidic chips for some tasks.<sup>2,3</sup> However, some physical phenomena in microfluidics do not have clear analogies in electrical circuits. Laminar flow, solute diffusion, sound,<sup>4</sup> light,<sup>5</sup> magnetism,<sup>6</sup> and gravity<sup>7</sup> all affect microfluidic chips in ways that are difficult to model using EDA techniques.

In this work we were motivated by the question, *is it possible to create functional microfluidic devices without actually designing them?* More precisely, what if we had a library of *all possible designs for microfluidic chips*, and creating a chip for a new application was as simple as searching through the library for the appropriate design? In this thought experiment, every possible application for microfluidics—from diagnosing diseases<sup>8</sup> to searching for life on Mars<sup>9</sup>—would have a suitable design in this library. If the behavior of each chip design was stored with the design in the library, then a researcher

<sup>a</sup> Department of Bioengineering, Bourns College of Engineering, University of California, Riverside, 900 University Ave, Riverside, CA, 92521, USA.

E-mail: [wgrover@engr.ucr.edu](mailto:wgrover@engr.ucr.edu); Tel: +1 951 827-4311

<sup>b</sup> Department of Computer Science and Engineering, Bourns College of Engineering, University of California, Riverside, 900 University Ave, Riverside, CA, 92521, USA

† Electronic supplementary information (ESI) available: An expanded version of Fig. 3 showing similar results from three solutes with different diffusion constants. See DOI: 10.1039/c6lc00758a

could merely search the library for chips with the desired behavior and fabricate and use these chips immediately, without actually designing the chips.

Obviously this hypothetical library of “all possible microfluidic chip designs” would be astronomically large. But it also raises some interesting possibilities. This library would undoubtedly contain chip designs that are far better than the designs created by humans for the same application. Microfluidics researchers have explored such a small fraction of this library of all possible designs—could there be entirely new and useful microfluidic phenomena waiting to be found in this hypothetical library?

While we cannot yet build a full library of “all possible chip designs,” we can still explore parts of this library. Specifically, by imposing constraints that limit the number of possible chip designs, we can in some cases actually test all possible chips, or at least explore enough random designs to catch a glimpse of the library of all possible chips. In this work we constrained our microfluidic chips to a rectilinear grid of channels shown in Fig. 1. We simulated the performance of over ten thousand different random chip designs based on this grid using FEA software, then created a database of the simulation results. We then queried this database to find chip designs suitable for given tasks. As a demonstration task, we instructed our software to select chip designs that take two fluids as inputs (one fluid, a solution with a known concentration of a solute; and the other fluid, water) and generate three output fluids with user-specified concen-

trations of the solute (like 92%, 66%, and 23%). We then fabricated and tested several of the chips selected by our software and used them to perform a cell growth rate assay. A graphical overview of our random design process is shown in Fig. 2. Despite not having been “designed” for any specific purpose, the selected chips successfully performed the desired tasks. This proof-of-concept is just one of many different applications for randomly-designed microfluidics; in principle, *any* microfluidic chip that can be simulated could be designed automatically using our method.

## 2 Results

### 2.1 Grid design

In this work we constrained our microfluidic chip designs to the rectilinear grid patterns shown in Fig. 1. An  $n \times n$  grid has  $n^2$  possible channel intersections and  $2n^2 - 2n$  possible channels connecting those intersections. If each of these connecting channels can be either present or absent in a given design, then the total number of different possible chip designs is  $2^{2n^2 - 2n}$ . If the size of the grid is small, it is feasible to generate all microfluidic chip designs that are possible within that grid. For example, the simplest grid we considered, a  $2 \times 2$  grid, has only  $2^{2 \times 2^2 - 2 \times 2} = 16$  different designs (Fig. 1A).

As a demonstration of randomly-designed microfluidics, we set out to find chips that are capable of generating any

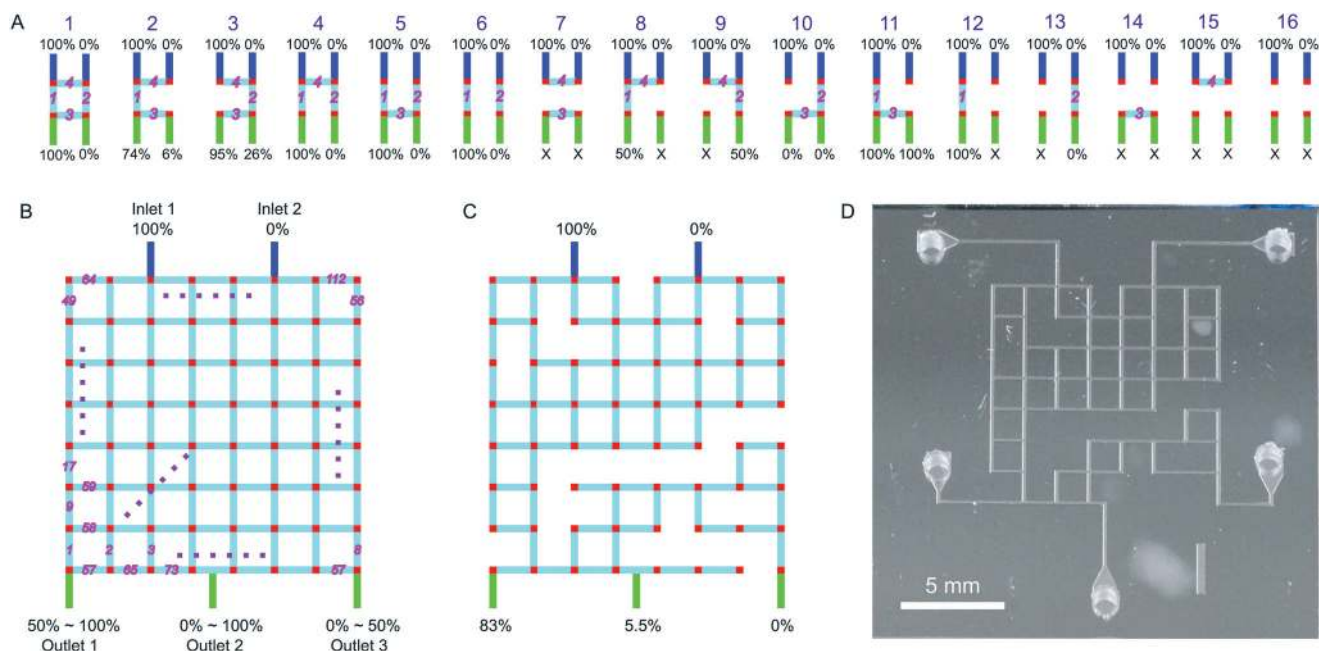


**Fig. 1** Surveying the library of “all possible microfluidic chip designs.” (A) For a microfluidic chip with two inlets (dark blue), two outlets (green), four channel intersections arranged in a square (red), and four possible channels connecting those intersections (light blue), there are  $2^4 = 16$  different chip designs. If solutions of concentrations 100% and 0% flow into the inlets at a constant volumetric flow rate, these 16 chip designs generate solutions with seven different specific concentrations at the outlets (0%, 6%, 26%, 50%, 74%, 95%, and 100%), and some designs generate no fluid (marked with “X”). (B) An  $8 \times 8$  grid supports  $2^{112} = 5 \times 10^{33}$  different chip designs that can generate essentially any three desired concentrations at the three outlets. One of these chip designs is shown in (C) and fabricated and photographed in (D); this specific design generates concentrations of 83%, 5.5%, and 0% at its outlets.

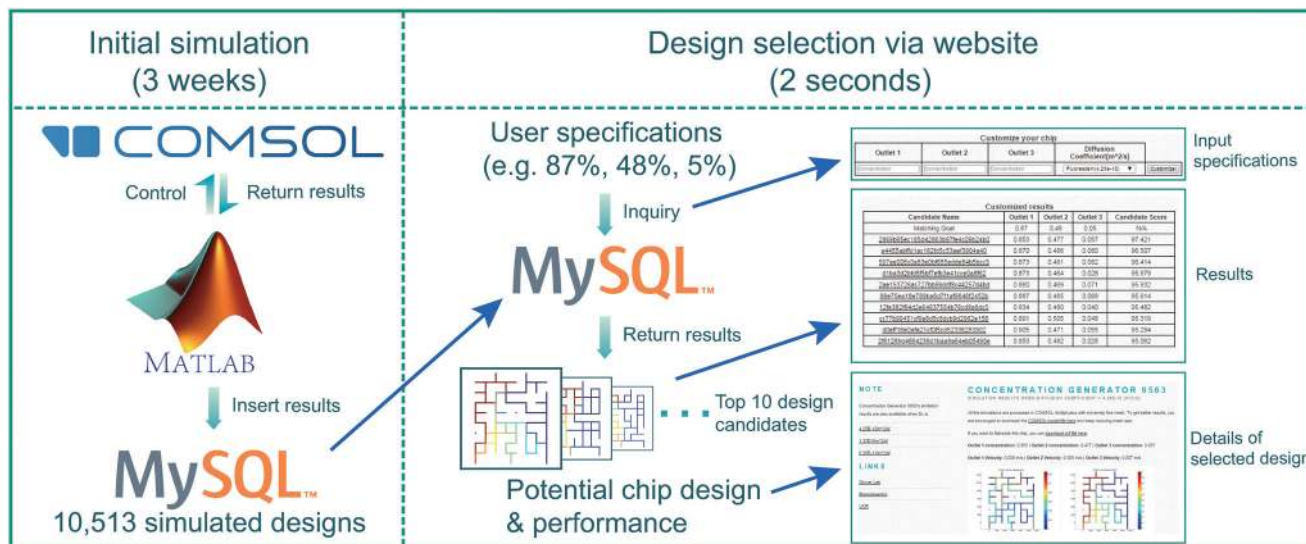


**Fig. 2** Overview of the random microfluidics design process. During the three-week initial simulation phase, a MATLAB program generated 10 513 random chip designs from the grid shown in Fig. 1B, simulated the performance of each design using the finite element analysis software COMSOL Multiphysics, and saved the simulation results to a MySQL database. This database of random chip designs was then transferred to a web server (<http://random.groverlab.org>) where a user can specify three desired solution concentrations. Within seconds, the website then returns the top ten chip designs that generate those concentrations, including simulation results and downloadable computer-assisted design (CAD) files for use in fabricating the chips.

three desired concentrations of a solute. Each chip design contains two inlet channels, one containing a 100% solution of a solute and one containing water (0% solute), flowing into the chip at a constant volumetric flow rate. As these fluid streams split and merge inside the chip, different mixtures of the two fluids are created. We then used finite element analysis (described below) to predict the concentrations of solute in each of the three outlet channels for each chip design.

In the 16 possible designs for the  $2 \times 2$  grid in Fig. 1A, four designs (7, 14, 15 and 16) have no connections between the inlets and outlets and thus output no fluid; four designs (1, 4, 5 and 6) output solute concentrations that are unchanged from the input concentrations (still 100% and 0%); two designs (10 and 13) output only 0%; two designs (11 and 12) output only 100%, two designs (8 and 9) output only 50%, one design (2) outputs solute concentrations of 74% and 6%; and one design (3) outputs solute concentrations of 95% and 26%. Thus, seven different specific solute concentrations (0%, 6%, 26%, 50%, 74%, 95%, and 100%) can be generated using chips from the  $2 \times 2$  library. If these seven concentrations are adequate for a given microfluidic application, then a user may select chip designs from this library and use them. However, if a user requires concentrations that are not generated by chips in the  $2 \times 2$  library, then a larger and more complex grid is necessary.

As the size of the grid grows larger, there are more opportunities for channel splits and merges that create different mixtures. We hypothesized that an  $8 \times 8$  grid would support a large enough variety of chip designs to ensure that any three desired mixtures will be generated by at least one design in the library. The  $8 \times 8$  grid in Fig. 1B supports  $2^{2 \times 8^2 - 2 \times 8} = 5, 192, 296, 858, 534, 827, 628, 530, 496, 329, 220, 096$  dif-

ferent chip designs, so clearly we will not be able to study every possible design. However, by randomly selecting thousands of designs from the  $8 \times 8$  grid and simulating their behavior, we can explore the variety of designs supported by this grid. And by fabricating and testing several of these designs, we can confirm that our technique of randomly-designed microfluidics can be used to select chip designs with desired behaviors.

## 2.2 Generating random microfluidic chip designs

A custom MATLAB program was written that generated 21 564 different random chip designs within the constraints of the grid design shown in Fig. 1B. Each of the 112 variable channels (light blue in Fig. 1B) has a 90% chance of being present in any given design. This value was chosen as a balance between two practical limits. If the probability of a channel being present is too low, many chip designs may not have a continuous path for fluid to flow between the inlets and outlets, rendering them nonfunctional. If the channel probability is too high, most chips will have nearly all variable channels present, leading to low diversity in the library of random designs. A 90% probability that each variable channel will be present seems to provide a good balance between encouraging functional devices and exploring a large fraction of the chip design space. Of the 21 564 different random chip designs, 10 513 designs have continuous paths for fluid between both inputs and all three outputs; these designs were retained for use in this study. 11 058 designs have paths for fluid between both inputs and two of the three outputs and were not used (although they could be used for applications requiring only two different concentrations of fluids).



### 2.3 Building the library of chip simulations

The behavior of each of the 10 513 random chip designs was simulated using the finite element analysis software COMSOL Multiphysics (COMSOL Inc., Burlington, MA). We used the software's MATLAB API<sup>10</sup> to automate this process and performed all simulations necessary to construct the library without human assistance. The results of each simulation included plots of fluid velocity, fluid pressure, and solute concentration at each point in the chip, as well as a COMSOL model file containing the simulation results. The two-dimensional simulations used 200  $\mu\text{m}$  channel widths, 1.5 mm channel lengths between vertices,  $1 \times 10^{-6}$  relative repair tolerance, and triangular meshes containing from  $5 \times 10^4$  to  $5 \times 10^5$  elements. In the *Laminar Flow* physics module in COMSOL Multiphysics, each inlet was assigned an inlet boundary condition of  $10 \text{ mm s}^{-1}$  normal inflow velocity, and each outlet was assigned an outlet boundary condition of 0 Pa pressure. The remaining boundaries were walls (no-slip boundary condition), and the material filling the channels was water under incompressible flow. In the *Transport of Dilute Species* physics module, inlet 1 is assigned an inflow of  $1 \text{ mol m}^{-3}$  and inlet 2 is assigned an inflow of  $0 \text{ mol m}^{-3}$ . The three outlets were assigned as outflows. Each chip design was simulated using the diffusion coefficients for sodium ions, fluorescein, and bovine serum albumin, as described below. Two stationary solvers were used in COMSOL Multiphysics: the first solved for laminar flow, and the second solved for transport of diluted species. After each simulation, the linear flow rates and solute concentrations at each of the three outlets were saved to a MySQL database. Additionally, the COMSOL model file, velocity profile, concentration profile, pressure profile, and a computer-assisted design (CAD) file containing the design of the chip in the standard DXF format<sup>11</sup> were saved to local storage. Users can query this database and download chip designs for specific applications at <http://random.groverlab.org>.

### 2.4 Role of diffusion in randomly designed chips

Solutes with different diffusion coefficients may result in different output concentrations in the same chip. To assess the role of diffusion and enable our library to support a wider variety of solutes, each chip design was simulated three times, once for each of three model solutes: sodium ions (diffusion coefficient  $D_c = 1.33 \times 10^{-9} \text{ m}^2 \text{ s}^{-1}$ ), fluorescein ( $D_c = 4.25 \times 10^{-10} \text{ m}^2 \text{ s}^{-1}$ ), and bovine serum albumin (BSA;  $D_c = 6.38 \times 10^{-11} \text{ m}^2 \text{ s}^{-1}$ ). These solutes were chosen to be representative of ions, small molecules, and proteins, respectively. The complete library of solute-specific simulations contains 31 515 simulation results and took three weeks to complete on a desktop computer.

### 2.5 Analyzing the random chip library

Before using our library of simulation results to generate chip designs for specific applications, we first analyzed the entire library to ascertain the range of microfluidic functions it sup-

ports. Fig. 3 shows the solute concentrations and fluid velocities at each of the three outlets for all 10 513 random chip designs (using the diffusion constant of fluorescein). The distribution of solute concentrations in Fig. 3 confirms that the library contains chip designs suitable for generating essentially any desired solute concentration.

Outlet 2 supports the widest variety of solute concentrations; designs yielding concentrations from 0% to 100% at outlet 2 are present in the library. Concentrations around 50% are most common at outlet 2, and 80% of the designs generate concentrations between 28% and 72% at outlet 2. These results make intuitive sense: as the middle outlet located halfway between inlet 1 (100%) and inlet 2 (0%), outlet 2 is well suited to yield a range of mixtures centered at 50%.

Outlet 1 yields a narrower range of solute concentrations (from 50% to 100%). The average concentration at outlet 1 is 95%, the median concentration is 98%, and 90% of the designs yield concentrations between 86% and 100%. These higher concentrations can be explained by the close proximity of outlet 1 to inlet 1 (which contains 100% solute); this close proximity favors designs in which most of the fluid from inlet 1 to flows to outlet 1 (and therefore increases the solute concentration at outlet 1).

Outlet 3 also yields a narrower range of solute concentrations (from 0% to 50%), with an average concentration of 5%, a median concentration of 2%, and 90% of the designs yielding concentrations between 0% and 15%. Again, the close proximity of outlet 3 to inlet 2 (which contains 0% solute) explains the preference for lower concentrations at outlet 1.

There is no obvious mathematical relationship between the fluid velocity and solute concentration at each of the three outlets in Fig. 3. Consequently, velocity and

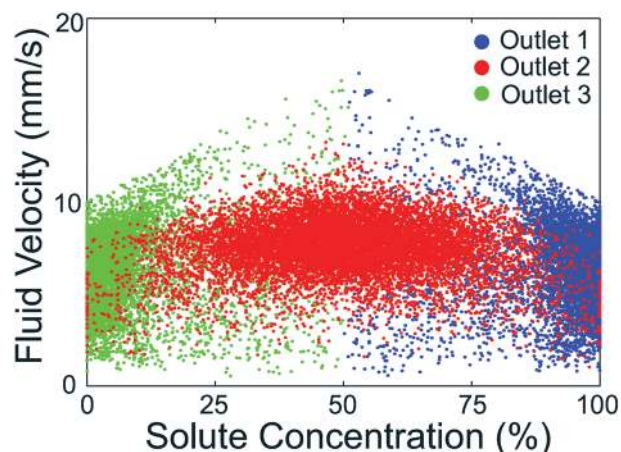


Fig. 3 Fluid velocity vs. concentration for each outlet in each of the 10 513 chip designs in our simulation library. While this data was obtained using the diffusion coefficient of fluorescein ( $4.25 \times 10^{-10} \text{ m}^2 \text{ s}^{-1}$ ), the results are essentially identical for solutes with larger or smaller diffusion coefficients (see online ESI<sup>†</sup>). The wide distributions of concentrations and velocities confirm that our proof-of-concept library can provide chip designs that generate any desired fluid concentrations at any desired flow rates up to approximately  $10 \text{ mm s}^{-1}$ .

concentration can be considered as independent variables when selecting designs from the library: a user could specify any desired concentration *and* any desired velocity and a suitable design is likely to exist within the library (at least over the ranges shown in Fig. 3).

We then identified which factors are most significant in determining the solute concentrations at the outlets. Specifically, fluids could be mixed by any of three different processes on-chip: the chip design (the various splits and merges fluids undergo in the chip), diffusion (mixing between adjacent streams of fluid in the chip), and turbulence (chaotic processes that also might mix fluids in the chip). At low flow rates, diffusional mixing would dominate, resulting in identical 50% concentrations at each outlet. At moderate flow rates, the effect of diffusion is reduced, and the mixing ratios would be determined by the channel network and the fluidic resistance of each channel segment. Finally, at high flow rates, the breakdown of laminar flow and emergence of turbulence could affect the mixing ratios in unpredictable ways. The dimensionless Péclet (Pe) and Reynolds (Re) numbers are used to determine in which of these regimes a microfluidic chip is operating:

$$\text{Pe} = \frac{Lu}{D} \quad (1)$$

$$\text{Re} = \frac{\rho Lu}{\mu} \quad (2)$$

where  $L$  is a characteristic dimension like channel width,  $u$  is the linear fluid flow rate,  $D$  is the solute diffusion constant,  $\rho$  is the density of the fluid, and  $\mu$  is the viscosity of the fluid. If  $\text{Pe} < 1$ , diffusion may have an effect on the mixing behavior of a chip, and if  $\text{Re} > 300$ , turbulence may have an effect on the mixing behavior. We calculated Re and Pe for each of the 10 513 random chip designs in our library. Values for Re at each location in each chip ranged from 0 to 6 and were all much lower than 300, indicating that no turbulent mixing is occurring in the chip designs. Typical values of Pe were 4500 for channels containing solutions of  $\text{Na}^+$ , 14 000 for fluorescein, and 94 000 for BSA; these are all much greater than 1 and indicate that diffusional mixing has a negligible effect on the outlet solute concentrations. These calculations suggest that chip design (and not turbulence or diffusion) is the primary determinant of the output solute concentrations over the range of flow rates we considered.

Finally, to determine if our library of chip designs can be used with a wide variety of solutes (not just the three whose behavior we simulated), we compared simulation results from the two solutes with the greatest difference in diffusion constants:  $\text{Na}^+$  and BSA. Even through the diffusion coefficient of  $\text{Na}^+$  is about 20 times larger than that of BSA, the average difference in outlet concentrations between  $\text{Na}^+$  and BSA for the 10 513 different designs in our library was only 1.02 percentage points, and the largest single difference in

outlet concentrations was only 2.76 percentage points. Additionally, versions of Fig. 3 containing the simulation results for all three solutes ( $\text{Na}^+$ , fluorescein, and BSA) are provided in online ESI;† they are essentially indistinguishable from each other. This further supports our claim that chip design (not diffusion) dominates the mixing behavior of the designs in our library over the range of flow rates we studied (from 0 to 10  $\text{mm s}^{-1}$  at the outlets), and our library contains designs that are suitable for generating solutions of any desired concentration using a wide variety of different solutes.

## 2.6 Selecting randomly-designed chips for specific tasks

We then transferred our database of 10 513 different random chip designs to a web server and created a website that allows users to search this database to find chips with desired behaviors. The website is available for public use at <http://random.groverlab.org>. After the user specifies the three desired solution concentrations, the website returns the design and simulation results for each of the top ten chip designs that will generate these concentrations. Note that this server does not run COMSOL or perform any simulations; it simply queries a database populated with simulation results.

To confirm that the chip designs selected by our website actually function as predicted, we chose 16 chip designs at random and fabricated glass microfluidic chips based on those designs. The only modification we made to the computer-generated designs was the deletion of all dead-end channels, which might trap bubbles during use and will have no effect on the mixing behavior of the chips. Conventional photolithography and wet etching were used to etch the randomly-designed chip designs into glass wafers to a depth of 50  $\mu\text{m}$ , inlet and outlet holes were drilled using diamond-tipped drill bits, and glass-glass thermal fusion bonding (668 °C for 6 hours) or anodic bonding to silicon (350 °C and 400 V for approximately 30 minutes) were used to create finished microfluidic devices.

The simulation results for these 16 designs (labeled A–P) are shown in Fig. 4, and a photograph of a chip fabricated using design L is shown in Fig. 1D. After fabricating chips for each of the 16 random designs in Fig. 4, we tested the performance of each chip by flowing a solution of  $1.0 \times 10^{-5}$  M fluorescein in 0.1 M Tris buffer (pH = 8.0) in inlet 1 and an identical solution without fluorescein in inlet 2. A two-channel syringe pump was used to provide a constant flow rate of 6  $\mu\text{L min}^{-1}$  at each inlet (this corresponds to a linear flow rate of 10  $\text{mm s}^{-1}$ ). After 10 minutes, fluid from each of the three outlets was collected for analysis. The fluorescein concentration of fluid from each outlet was measured using a FlexStation microplate reader (Molecular Devices, Sunnyvale, CA) using an excitation wavelength of 490 nm and an emission wavelength of 514 nm.

Fig. 5A–D compares our experimental results with the values predicted by our simulation library. The average percent difference between the predicted and experimental values of concentration at each outlet was 2% for outlet 1, 4% for outlet 2, and 0.3% for outlet 3. The greatest single

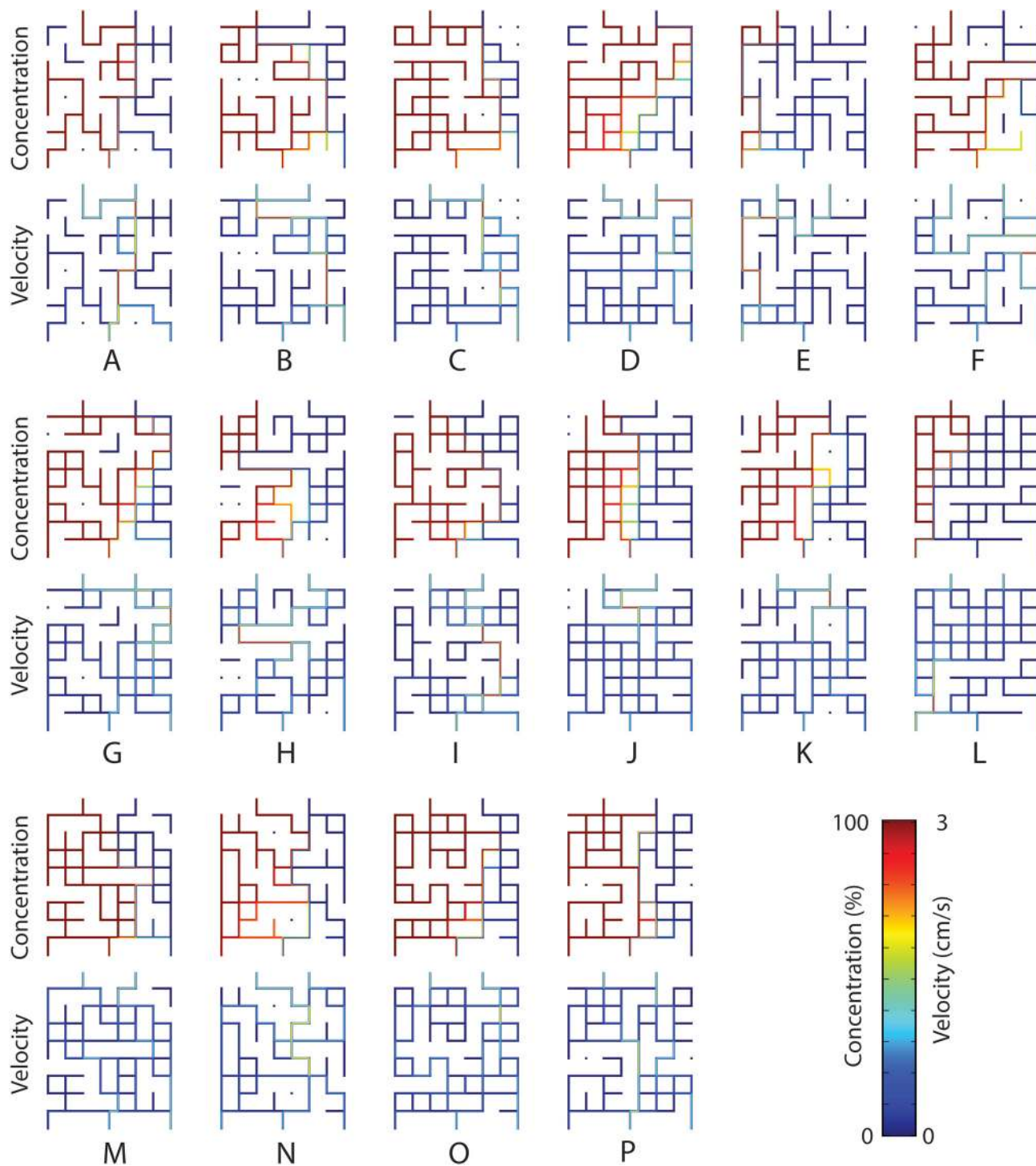


Fig. 4 Simulation results for 16 chip designs (A–P) selected at random from our library of 10 513 random chip designs, using the diffusion coefficient of fluorescein ( $4.25 \times 10^{-10} \text{ m}^2 \text{ s}^{-1}$ ). As the channels split and merge in the random designs, the constant solute concentrations (100% and 0%) and constant fluid flow rates ( $6 \mu\text{L min}^{-1}$ ) at the inlets translate into a variety of different concentrations and flow rates at the outlets.

difference between predicted and experimental values was at outlet 2 on chip P (9% difference). These differences between predicted and experimental results compare favorably with other microfluidic mixers<sup>12</sup> and are low enough for many microfluidic applications.

Finally, we also used our randomly-designed microfluidic chips to automatically generate five different concentrations

of cell media for use in a cell growth assay. We selected three chips (A, G, and H) that generated 5%, 10%, 57%, 83% and 99% concentrations of yeast growth media. On each chip, inlet 1 received 100% yeast extract peptone dextrose media (YPD; Thermo Fisher Scientific, Waltham, MA USA) and inlet 2 received water. 10 mL of media from each outlet was collected into test tubes that were then inoculated with identical amounts



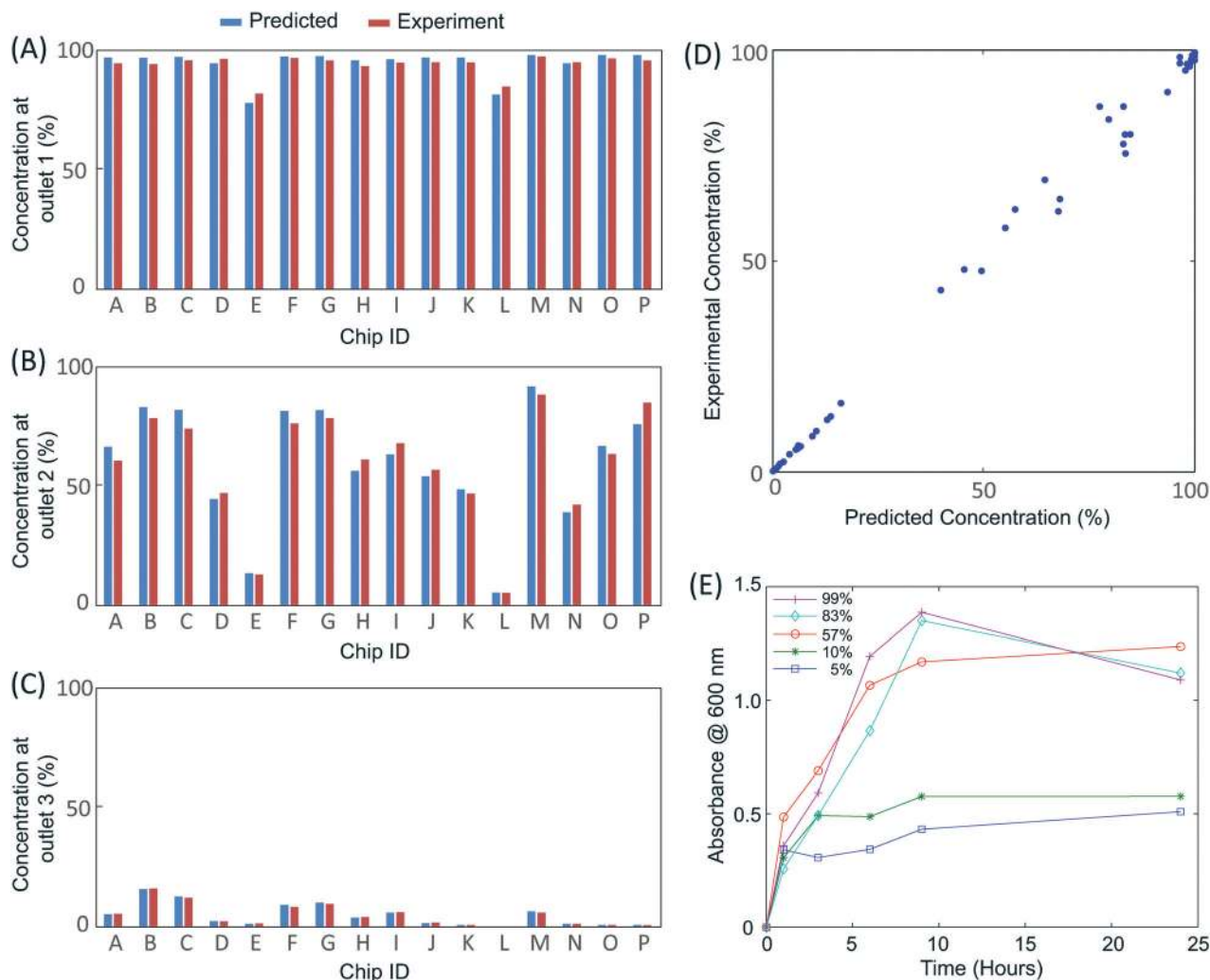


**Fig. 5** (A–D) Comparisons between the predicted and experimentally-determined performance of each of the 16 randomly-designed test chips shown in Fig. 4. The solute concentrations predicted by our library (blue) agree well with the measured concentrations (red) for each chip at outlet 1 (A), outlet 2 (B), and outlet 3 (C). When combined (D), all 48 solute concentrations generated by these 16 chips are consistent with the library predictions over the full range of concentrations from 0% to 100%. (E) To demonstrate that randomly-generated microfluidic chips can perform real-world biological applications, three chips were used to automatically generate five different concentrations of cell culture media (5%, 10%, 57%, 83% and 99% of yeast extract peptone dextrose). The optical absorbance at 600 nm was measured to obtain growth curves of *Saccharomyces cerevisiae* yeast in each media concentration generated by the randomly-designed chips. As expected, yeast cultures with lower media concentrations reached steady state earlier and with a smaller number of cells than cultures with higher media concentrations.

of *Saccharomyces cerevisiae* yeast and cultured at 25 °C for 24 hours. Growth curves for each culture were obtained by periodically measuring the optical absorbance at 600 nm using an UV-vis-NIR spectrophotometer (V-670, Jasco, Easton, MD).

Yeast growth curves (Fig. 5E) show that while the initial growth rates were fairly comparable for all five media concentrations generated by our randomly-designed chips, yeast in the lowest-concentration media (5% and 10%) exhausted their nutrients and entered stationary phase earlier and with fewer cells than the yeast in the higher-concentration media. Growth curves like these play an important role in studies of human conditions like aging and cancer,<sup>13</sup> and our randomly-designed chips could replace manual labor or expensive computer-controlled valves and pumps in an instrument for automated measurement of growth curves. These results sug-

gest that randomly-generated microfluidic chips *can* support real-world research applications.

### 3 Discussion

We demonstrated how to create functional microfluidic chips for specific applications without actually designing the chips. We accomplished this by generating a large library of random chip designs, simulating their behavior using finite element analysis, and saving the results in a database that can be queried by users *via* a website. Using this website, researchers with no experience in designing microfluidics can easily find chip designs that satisfy their own unique needs.

As a proof-of-concept, we created a library of 10 513 random chip designs that can generate three solutions of any



desired concentrations. These random chips have several unique properties compared to existing chips for generating solutions with different concentrations. First, while most existing chips rely on diffusion to create a range of different solute concentrations,<sup>14–16</sup> our randomly-designed chips use only the series of channel splits and merges in the chip to generate different concentrations. Consequently, our randomly-designed chips can be operated over a wider range of flow rates than chips that rely on diffusion, and users can specify both the desired concentration *and* the desired flow rate at each outlet. Additionally, while microfluidic valve- and pump-based serial diluters generate waste fluids with undesired concentrations during operation,<sup>17,18</sup> our randomly-designed chips generate only fluid with the desired concentrations and create no waste fluid. These differences show that randomly-generated microfluidic chips can have unexpected and useful advantages over their human-designed counterparts.

Finally, our technique can be used to find microfluidic chip designs that do more than simply generate solutions with user-specified concentrations. Any microfluidic phenomenon that can be simulated could be the basis for a library of chip designs and simulations that could subsequently be queried by users for a wide variety of different applications. For example, a library of random chip designs whose simulations include two-phase flow (oil and water) could be used to automatically design microfluidic droplet generators, and a library whose simulations include particle tracing could be used to automatically design cell sorters. Generating these libraries may require a non-trivial amount of computation time: our proof-of-concept library required three weeks to complete. However, that library was generated using an ordinary desktop computer, and higher-performance hardware could speed up library generation considerably. As libraries of random chip designs proliferate in the future, even complex lab on a chip devices for important research and healthcare applications could be created in seconds without actually designing them.

## Acknowledgements

The authors thank George Way and Dr. Jiayu Liao in the Bio-engineering Department at UC Riverside for their assistance. This work was supported in part by the National Science Foundation Division of Biological Infrastructure under award

DBI-1353974 and the National Science Foundation Division of Computer and Communication Foundations program under awards CCF-1351115 and CCF-1536026.

## References

- 1 S. C. Terry, J. H. Jerman and J. B. Angell, *IEEE Trans. Electron Devices*, 1979, **26**, 1880–1886.
- 2 J. McDaniel, B. Crites, P. Brisk and W. H. Grover, *IEEE Des. Test*, 2015, **32**, 51–59.
- 3 H. Yao, Q. Wang, Y. Ru, Y. Cai and T.-Y. Ho, *IEEE Des. Test*, 2015, **32**, 60–68.
- 4 J. Friend and L. Y. Yeo, *Rev. Mod. Phys.*, 2011, **83**, 647.
- 5 C. Monat, P. Domachuk and B. Eggleton, *Nat. Photonics*, 2007, **1**, 106–114.
- 6 N. Pamme, *Lab Chip*, 2006, **6**, 24–38.
- 7 N. Norouzi, H. C. Bhakta and W. H. Grover, *PLoS One*, 2016, **11**, e0149259.
- 8 P. Yager, T. Edwards, E. Fu, K. Helton, K. Nelson, M. R. Tam and B. H. Weigl, *Nature*, 2006, **442**, 412–418.
- 9 A. M. Skelley, J. R. Scherer, A. D. Aubrey, W. H. Grover, R. H. Ivester, P. Ehrenfreund, F. J. Grunthaler, J. L. Bada and R. A. Mathies, *Proc. Natl. Acad. Sci. U. S. A.*, 2005, **102**, 1041–1046.
- 10 *LiveLink for Matlab*, <https://www.comsol.com/livelink-formatlab>, Accessed: 2016-03-23.
- 11 *ASCII DXF Files*, <http://www.autodesk.com/techpubs/autocad/acad2000/dxf/ascii-dxf-files-dxf-aa.htm>, Accessed: 2016-09-26.
- 12 M. A. Holden, S. Kumar, E. T. Castellana, A. Beskok and P. S. Cremer, *Sens. Actuators, B*, 2003, **92**, 199–207.
- 13 L. Galdieri, S. Mehrotra, S. Yu and A. Vancura, *OMICS*, 2010, **14**, 629–638.
- 14 K. Lee, C. Kim, B. Ahn, R. Panchapakesan, A. R. Full, L. Nordee, J. Y. Kang and K. W. Oh, *Lab Chip*, 2009, **9**, 709–717.
- 15 D. Irimia, D. A. Geba and M. Toner, *Anal. Chem.*, 2006, **78**, 3472–3477.
- 16 N. L. Jeon, S. K. Dertinger, D. T. Chiu, I. S. Choi, A. D. Stroock and G. M. Whitesides, *Langmuir*, 2000, **16**, 8311–8316.
- 17 F. K. Balagaddé, L. You, C. L. Hansen, F. H. Arnold and S. R. Quake, *Science*, 2005, **309**, 137–140.
- 18 B. M. Paegel, W. H. Grover, A. M. Skelley, R. A. Mathies and G. F. Joyce, *Anal. Chem.*, 2006, **78**, 7522–7527.